ISSN: 0974-5823 Vol. 7 No. 4 April, 2022

International Journal of Mechanical Engineering

EFFECT OF DOPING (Cd, Dy) OPTICAL PROPERTIES OF STO CERAMICS

V. Ratchagar*, A. Vishnupriya, R. Shirly, V. Vaishnavi, A. Muthuraja

*Department of Physics, Theivanai Ammal College for Women (Autonomous), Villupuram, Tamil Nadu. India

Abstract

STO with different dopant Cd, Dy was prepared by solid-state technique. XRD shows the formation of simple perovskite structure with "Pm-3m" space group of all the synthesized samples. A Fourier Transform IR spectrum confirms the metal oxide chemical bonding present in the compounds. Poly dispersed behaviour was recognized through SEM micrographs. EDX spectra confirm the presence of (Sr, Ti, O, Cd) elements. The bandgap values were estimated through UV-Visible studies. From the PL spectra, the existence of tri-colour emission at an excitation of 330 nm was observed. Dielectric constant, loss depend on temperature and frequency.

Keywords: STO, Cd, Dy, Solid state reaction method, Dielectric studies.

Introduction

A perfect cubic unit cell is only present within $SrTiO_3$ oxides with general formula ABO_3, where A is either alkali or alkaline earth or rare earth elements and B is either transition metal or fourth group elements, are known as Perovskite oxides [1-3]. Owing to their high thermal stability, excellent oxidation activity, and low price, perovskites have been explored for a variety of environment-related and energy-related applications, including automobile exhaust purification, fuel cells, N_2O decomposition and water–gas shift reactions [4]. $SrTiO_3$ has an indirect band gap of 3.25 eV and a direct band gap of 3.75 eV [5]. Strontium^{2+} ions and oxygen^{2-} ions are exhibiting an ionic bonding. Within the TiO_6 octahedra, while a hybridization of the Oxygen-2p states with the Titanium-3d/4f states leads to a pronounced covalent bonding. Hence, $SrTiO_3$ has mixed ionic-covalent bonding properties.

Recently, Mn doped $SrTiO_3$ increases the dielectric permittivity magnitude that pushes the device away from ferroelectric instability. Fe-doped $SrTiO_3$ exhibit saturated ferromagnetic transition in the annealed samples of x = 0.1 and 0.15 is due to the influence of Fe metal [92]. A blocking electrode was used to investigate the effect of iron (Fe) doping material on electrical conductivity, namely ionic & electronic conductivities, and the conduction activity of $Y_{0.08}\,Sr_{0.92}\,Ti_{1-x}\,Fe_x\,O_{3-\delta}$ with temperature [6-7]

In prior investigation, various elements (dopants) have been utilized to control the particle size, magnetic, dielectric and optical behaviour of STO mixes. In addition, there are frightening records available for STO doped with cadmium. In the current research, therefore, cadmium oxide and Dysprosium is chosen as a dopant which is wide-ranging applications in numerous areas such as panel display, solar cells, transparent, gas sensors, phototransistors, optical communicator. Hence, the aim of this present study was to explore the electrical, optical, structural and magnetic properties of Cd and Dy doped $SrTiO_3$ compound prepared by SSR technique.

EXPERIMENTAL PROCEDURE

Sample Preparation

Fine crude powders Strontium carbonate ($SrCO_3$), titanium dioxide (TiO_2) and cadmium oxide (CdO) and (Dy_2O_3) of analytical reagent (AR) grade were utilized to create $Sr_{1-x}\,Cd_x\,TiO_3$ through solid state procedure with the proportion of x= (0.05 Wt. %). As expressed by the stoichiometric amount with different x estimations of Cd- and Dy doped $SrTiO_3$ were pre-warmed at 200^o C for 1 hour. The powders were ground pleasantly in an agate mortar utilizing C_3H_6O as dissolvable for 60 minutes, at that point dried for 6 hours at 400^o C and calcined for 6 hours at 1000^o C.

RESULTS AND DISCUSSION

Structural Analysis

The XRD pattern of the STO with various dopant concentration of CdO is displayed in Figure 3.1. The observed diffraction peak positions and their corresponding diffraction peaks planes are indexed in the XRD pattern, which is perfectly matched with the standard JCPDS (Card No: 01-084-0443) [8] of STO. Based on the above diffraction peak positions, the synthesized CdO and Dy doped STO samples confirmed the formation of cubic structure with space group (Pm-3m). The diffraction pattern, Cd and Dy doped samples displays a traceable amount of auxiliary peaks with intensity Anyway, those peaks were exceptionally little and a rise because of the physical nature of Cd and Dy particles and as they were set up at high temperature.

The crystal size of the as-prepared powders were calculated using Scherrer formula

$$D = \frac{K\lambda}{\beta COS\theta}$$

Where, D is the crystal size,

λ is the X-ray wavelength, (CuKα - 1.5406 Å)

β is the full width at half maximum of the diffraction peak, and

θ is the Bragg diffraction angle of corresponding peaks.

S.No	Sample Name	Crystal Size (nm)
1.	STO	31
2.	Cd	43
3.	Dy	24

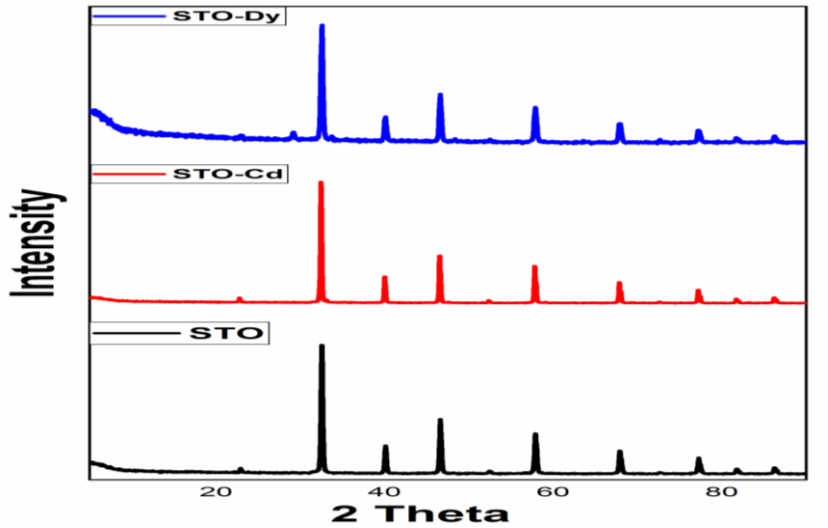

Fig: 1 Powder X-Ray Diffraction

FT-IR Studies

Figure 3.3 displays the FT-IR spectra of pure and CdO doped $SrTiO_3$ compounds. The functional group of the synthesized product can be confirm using the obtain bands in the FTIR spectra. The IR groups beneath 1000 cm^{-1} was ascribed to the Ti-O deformation modes in TiO_6 octahedra or because of the occurrence of Ti-O-Ti deformation [9]. The broad bands were observed between the range of 450 and 750 cm^{-1}, which indicates that the formation of metal oxide bond (Sr-O/Ti-O/Cd-O/Dy-O) [5]. The presence of bands at 1461 and 1327 cm^{-1} attributes to the carbonates present in the samples [10-13].

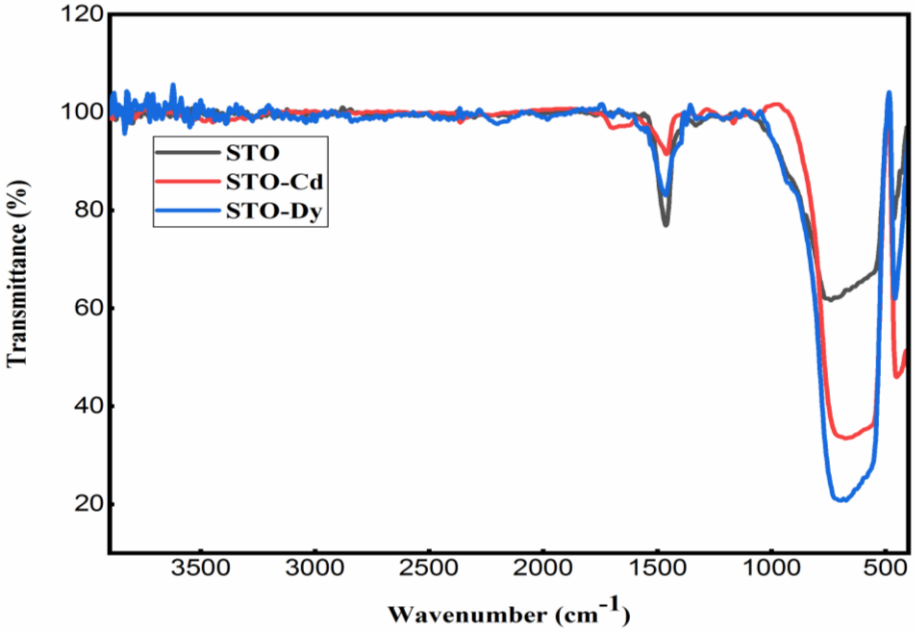

Fig 2. FTIR analysis

SEM analysis

Figure shows the scanning electron microscope of pure $SrTiO_3$ and CdO / Dy - doped $SrTiO_3$ samples. It could be seen that the pure $SrTiO_3$ and CdO-doped $SrTiO_3$ samples were observed agglomerated and poly-dispersed particles in the SEM images. As the CdO dopant concentration, the grain size elevates slowly. Dy-doped $SrTiO_3$ compounds. It's evident that the particles were irregular in shape with decreased grain size. Also, the particles were agglomerated/clustered formation was obtained.

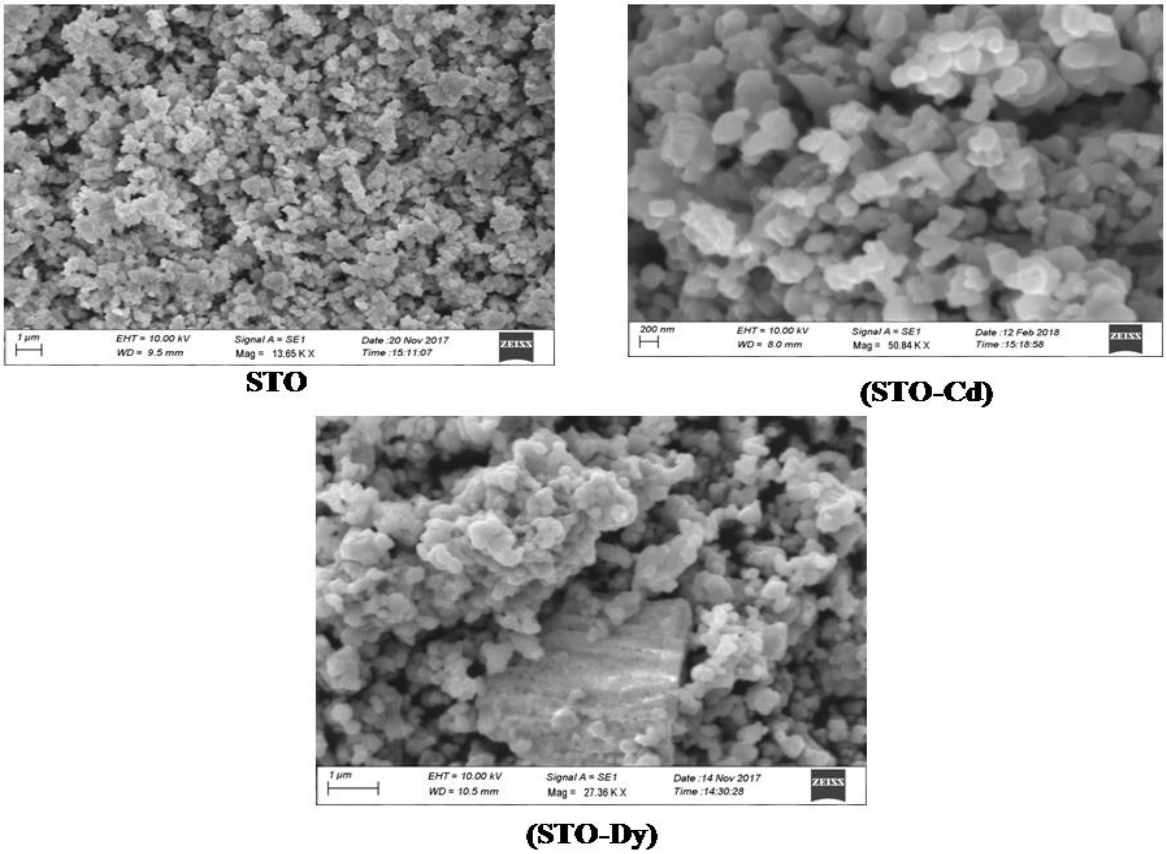

Fig 3: SEM Analysis

UV-Vis absorption spectra

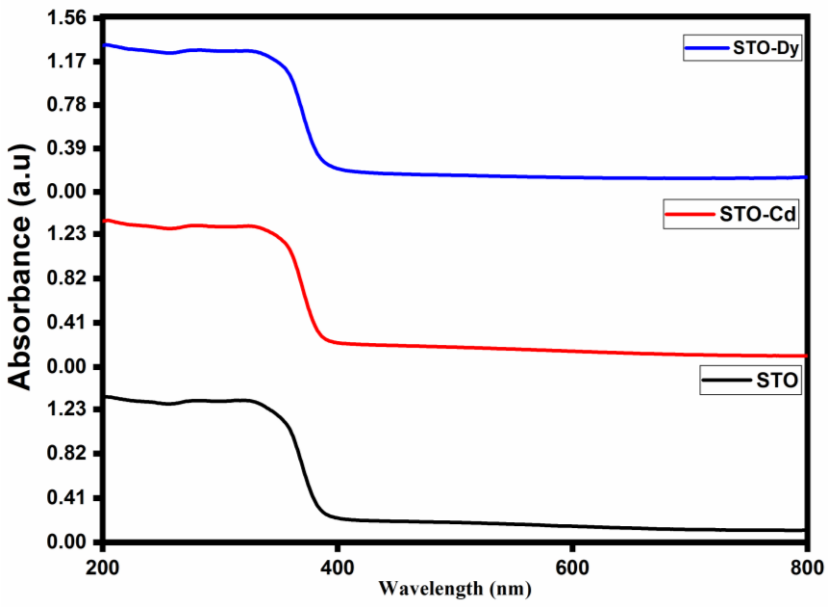

Fig 4 UV spectrum analysis

UV-Vis absorption spectra of the pure and Cd, Dy doped $SrTiO_3$ samples were displayed in Figure The cut off wavelength for pristine STO was detected to be 330 nm in the UV-visible spectra. The optical absorption was detected towards to the higher frequency side with raising the dopant Cd in the STO samples compared to that of pristine STO. In addition, it suggests the strong optical absorption activity for the Cd doped $SrTiO_3$ samples. The overall absorption was interpreted as transposing towards the higher frequency side, while raising the dopant Dy in STO lattice. The strong optical absorption character of pristine STO is attributed to the transition between oxygen- 2p and titanium- 3d / 4f states.

Photoluminescence Analysis

Figure shows the photoluminescence activity of synthesized pure $SrTiO_3$ and Cd-doped $SrTiO_3$ samples by applying an excitation wavelength of 330 nm. Emissions are violet, blue and green. PL's effectiveness on semiconducting samples depends on the materials preparation techniques, sintering temperatures, reaction time, particle size and morphology [12]. Two peaks at 374 and 383nm with low intensity and wavelength indicating that the electron-hole recombination is less, furthermore there was a shift in the pinnacle position of Dy doped samples towards higher intensity.

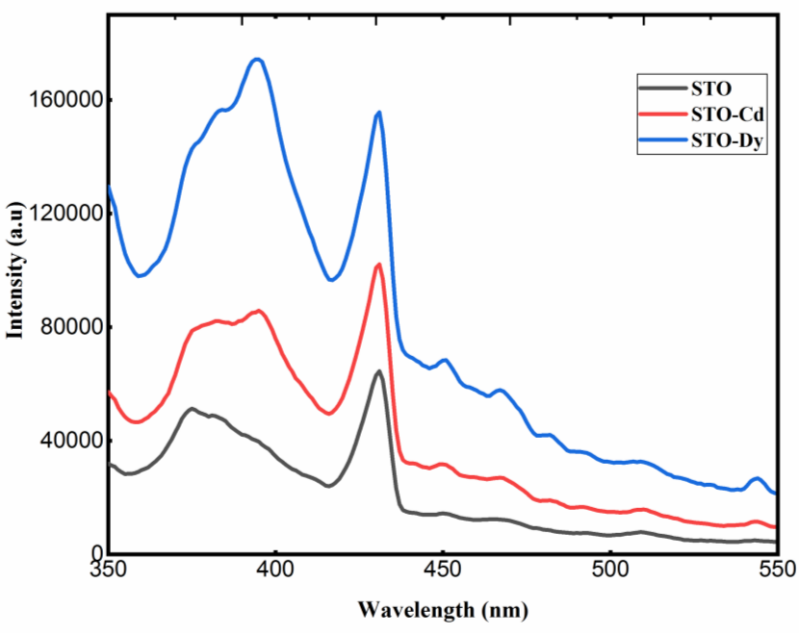

Fig 5 Photoluminescence analysis

Conclusion

The effect of a dopant such as Cd, Dy Strontium Titanate ($SrTiO_3$) perovskite structured compounds was investigated. Pure $SrTiO_3$ and Cd, Dy doped $SrTiO_3$ were prepared by solid state reaction method. All the dopants induced changes in the host lattice, among these dopants, In an overview, all the dopants seem to interact with the host lattice and induce a change in morphology along with the local disorder. It is seen that the dopants strongly influence the electronic structure and it could have the ability to tune the optical studies Hence from the present investigations, the physical nature of dopants, preparation technique, calcination temperature, doping level and morphological difference plays an important role in defining structural, optical properties.

Reference

[1] P. Esther Rubavathi, M. Veera Gajendra Babu, B. Bagyalakshmi, L. Venkidu, D. Dhayanithi, N.V. Giridharan, B. Sundarakannan, Impact of Ba/Ti ratio on the magnetic properties of BaTiO3 ceramics, Vacuum, 2019. https://doi.org/10.1016/j.vacuum.2018.10.063.

[2] I.N. Apostolova, A.T. Apostolov, Safa Golrokh Bahoosh, Julia M. Wesselinowa, Origin of ferromagnetism in transition metal doped BaTiO3, J. Appl. Phys. 113 (2013), 203904. https://doi.org/10.1063/1.4807412.

[3] H. Yanhong, L. Huibin, G. Haizhong, L. Lifeng, H. Meng, C. Zhenghao, Z. Yueliang, Z. Kun, J. Kuijuan, Y. Gouzen, Structure and electrical characteristics of Nb-doped SrTiO3 substrates, Chin. Sci. Bull. 51 (2006) 2035–2037, https://doi.org/10.1007/s11434-006-2075-3.

[4] Jie Hu, Liang Zhang, Benqian Lu, Xueqian Wang, Hao Huang, LaMnO3 nanoparticles supported on N doped porous carbon as efficient photocatalyst, Vacuum 159 (2019) 59–68, https://doi.org/10.1016/j.vacuum.2018.10.021.

[5] M. Muralidharan, V. Anbarasu, A. Elaya Perumal, K. Sivakumar, Carrier mediated ferromagnetism in Cr doped SrTiO3 compounds, J. Mater. Sci. Mater. Electron. 26 (2015) 6352–6365, https://doi.org/10.1007/s10854-015-3223-9.

[6] M. Valant, T. Kolodiazhnyi, I. Arc, F. Aguesse, A.K. Axelsson, N.M. Alford, The origin of magnetism in Mn-doped SrTiO3, Adv. Funct. Mater. 22 (2012) 2114–2122. https://doi.org/10.1002/adfm.201102482. [7] M.-S. Zhang, Z. Yin, Q. Chen, W.F. Zhang, W.C. Chen, Study of structural and photoluminescence properties in barium titanate nanocrystals synthesis by hydrothermal process, Solid State Commun. 119 (2001) 659–663. https://doi. org/10.1016/S0038-1098(01)00312-X.

[8] Y. Mao, S. Banerjee, S.S. Wong, Large-scale synthesis of single-crystalline perovskite nanostructures, J. Am. Chem. Soc. 125 (2003) 15718–15719, https:// doi.org/10.1021/ja038192w. [9] H. Herrig, R. Hempelmann, A colloidal approach to nanometer-sized mixed oxide ceramic powders, Mater. Lett. 27 (1996) 287–292. https://doi. org/10.1016/0167-577X(96)00011-0.

[10] X. Wu, D. Wu, X. Liu, Negative pressure effects in SrTiO3 nanoparticles investigated by Raman spectroscopy, Solid State Commun. 145 (2008) 255–258. https://doi. org/10.1016/j.ssc.2007.11.018. [11] T. Ahmad, A.K. Ganguli, Reverse micellar route to nanocrystalline titanates (SrTiO3, Sr2TiO4, and PbTiO3): structural aspects and dielectric properties, J. Am. Ceram. Soc. 89 (2006) 1326–1332. https://doi.org/10.1111/j.1551-2916.2005.00 886.x.

[12] B.V. Prasad, G. Narsinga Rao, J.W. Chen, D. Suresh Babu, Abnormal high dielectric constant in SmFeO3 semiconductor ceramics, Mater. Res. Bull. 46 (2011) 1670–1673, https://doi.org/10.1016/j.materresbull.2011.06.001.

[13] Reema Gupta, Vinay Gupta, Monika Tomar, Structural and dielectric properties of PLD grown BST thin films, Vacuum 159 (2019) 69–75, https://doi.org/10.1016